



A Quantitative Microbial Risk Assessment (QMRA) framework for exposure from toilet flushing using experimental aerosol concentration measurements

Ciara A. Higham^{a,*}, Martín López-García^b, Catherine J. Noakes^c, Emma Tidswell^c, Louise Fletcher^c

^a EPSRC Centre for Doctoral Training in Fluid Dynamics, University of Leeds, Woodhouse Lane, Leeds LS2 9JT, United Kingdom

^b School of Mathematics, University of Leeds, Woodhouse Lane, Leeds LS2 9JT, United Kingdom

^c School of Civil Engineering, University of Leeds, Woodhouse Lane, Leeds LS2 9JT, United Kingdom

ARTICLE INFO

Keywords:

QMRA
Toilet
Aerosols
Infection risk

ABSTRACT

Background: Flushing a toilet generates aerosols potentially containing microorganisms, serving as a transmission route for pathogens, notably gastrointestinal and respiratory infections. Despite identification of aerosols and positive microbial sampling, there is a lack of quantitative assessments linking aerosol generation to infection risk in toilet settings.

Methods: We develop a framework to evaluate the infection risk to a second susceptible individual using a shared toilet following faecal shedding and flush aerosolisation by an infected individual. Experimental measurements of particle concentrations from a toilet flush in a controlled chamber are combined with a model using Quantitative Microbial Risk Assessment (QMRA) methods. We demonstrate the approach for SARS-CoV-2 and norovirus, examining model sensitivity and how adding cubicle space and varying occupancy times affect risk.

Results: The model suggests non-negligible infection risk from the toilet plume, particularly for pathogens with higher concentrations in faeces. The model suggests norovirus could have a 2 times greater maximum infection risk than SARS-CoV-2. Mean and median risks for all scenarios decreased when the second individual entered 60 s post-flush compared to 0 s. Occupancy times had less impact on risk compared to the timing of entry post-flush.

Conclusion: To mitigate infection risk from shared toilets, ventilating the room before entering is crucial. Allowing time between toilet usages may be more effective compared to reducing occupancy times. Models provide valuable insights into relative impacts of measures and comparison between pathogens, but improved quantitative data is needed, particularly in higher risk scenarios (e.g. hospitals, public events), to quantify absolute risks.

1. Introduction

Droplets and aerosols are produced through the act of flushing the toilet, known as the toilet plume. They can contain microorganisms as large as bacteria, and their particle sizes are capable of penetrating the lower respiratory tract [1–3]. Such bioaerosols can remain viable and airborne for extended periods of time, with one study showing bacteria could be cultured after 4–6 hours [4]. They can migrate well away from the toilet facility and settle on surfaces throughout a bathroom, contaminating the surfaces [1,4]. One study found that up to 145,000

aerosols can be produced per flush, with the majority of measured particles having diameter less than 5 μm [5].

This has implications for pathogens transmitted via the faecal-oral route, and potentially for respiratory viruses if they are shed in faeces. This is of particular concern in settings where people are more vulnerable; a point-prevalence survey of healthcare-associated infections (HAIs) in European acute care hospitals found respiratory infections and gastrointestinal infections to account for 25.7 % and 8.9 % of HAIs respectively [6]. In addition, toilet facilities in UK healthcare settings do not usually have lids. There are varying views on whether toilet lids

* Corresponding author.

E-mail address: sccah@leeds.ac.uk (C.A. Higham).

<https://doi.org/10.1016/j.indenv.2024.100069>

Received 22 October 2024; Received in revised form 3 December 2024; Accepted 14 December 2024

Available online 16 December 2024

2950-3620/© 2024 The Authors. Published by Elsevier Inc. on behalf of International Society of Indoor Air Quality and Climate. This is an open access article under the CC BY license (<http://creativecommons.org/licenses/by/4.0/>).

influence transmission via the toilet plume. One study suggested that lidless toilets increase airborne and surface contamination, finding an increased risk for *C. difficile* for a lidless toilet [7]. Another recent study reported that closing the lid before flushing a toilet filled with a bacteriophage MS2 solution did not reduce the viral contamination of bathroom surfaces [8].

When people enter a shared toilet facility, they may be exposed to pathogens dispersed via the toilet plume from a previous occupant in several ways: airborne, surface and close-range exposure. For airborne exposure, droplets typically less than 100 μm evaporate rapidly, to create droplet nuclei [9,10]. The droplet nuclei can potentially contain infectious pathogens, remain airborne for minutes or hours and may be inhaled. Surface exposure occurs when surfaces become contaminated either by i) larger droplets ($> 100 \mu\text{m}$) that travel ballistically due to gravity or ii) smaller droplets ($< 100 \mu\text{m}$) that impact surfaces due to external airflows (i.e., ventilation) before full evaporation. A person may then touch the surface and subsequently touch their nose, mouth or eyes and become infected. Close-range exposure happens when an individual is infected at close proximity to a source and can be a combination of inhaled small aerosols or ballistic droplets that strike the mouth, nose or eyes of an individual [11].

There are multiple epidemiological studies showing evidence for airborne transmission of viruses in toilet facilities and bathroom settings. A healthcare outbreak of COVID-19 in Korea in 2020 was linked to airborne transmission, possibly due to a poor ventilation system and an unintended positive air pressure in the bathroom [12], though it is not clear whether aerosols from a toilet or a respiratory source were involved. In 2003, an outbreak of SARS1 at a Hong Kong residential complex, Amoy Gardens, led to 341 cases and resulted in 42 deaths [13]. This was most probably due to a defective U-trap in the building sanitation system. It was hypothesised, through both spatial and temporal analyses and Computational Fluid Dynamics (CFD) analyses, that aerosolisation of pathogens released via faeces in the sanitary plumbing system led to the infection of individuals in separate apartments to that of the infected individual. A similar, but smaller scale, outbreak happened during the COVID-19 pandemic in 2020 where there was evidence for aerosol transmission of faecal matter in a high-rise building in China [14]. This outbreak saw nine people becoming infected, and again it was likely due to aerosolisation of faecal matter which entered apartments through vents. A norovirus outbreak occurred on board a flight from London to Philadelphia in 2002 [15], where 8 of 14 flight members had experienced vomiting or diarrhoea in-flight, with no cases reported in those who didn't use the bathroom. Passengers who became infected had visited the toilet facility more often, suggesting the possibility of aerosol or surface transmission. In 1988, an outbreak of viral gastroenteritis aboard a transatlantic cruise ship occurred [16]. Twice as many people infected had used a shared bathroom in comparison to those with a private bathroom.

Evidence for secondary pathogen transmission in households has been documented [17–20]. For SARS-CoV-2, secondary attack rates in households have been estimated to be 5 – 10 times greater than in non-household settings [21]. With toilet facilities being a main feature in many households, this may be a particularly important environment to consider when assessing secondary transmission risks in households.

While substantial evidence exists detecting viral SARS-CoV-2 RNA copies in faecal matter, there is less evidence to confirm whether this corresponds to infectious virus. Although limited, there are studies which have cultured infectious virus from the stool or rectum of humans and animals. A systematic review on faecal-oral transmission of SARS-CoV-2 [22] identified 13 studies reporting successful infection when inoculating cells, tissues, organoids, or animals in vivo with faecal SARS-CoV-2. Of these, 2/13 studies used rectal swabs [23,24] and 11/13 used faecal matter [25–35], with 9/13 using human samples [25–28,30, 32–35], and 4/13 [23,24,29,31] using samples from various animal species. However, there is no evidence to date of viable SARS-CoV-2 persisting in wastewater, leaving the associated risk uncertain. Based

on the current evidence, this potential risk cannot be disregarded and has been accounted for in this study.

The toilet plume exists and has been illustrated visually using laser imaging techniques [36]. However, despite identification of aerosols and positive sampling for microorganisms there has not been any prior attempt to quantitatively relate the amount of aerosol generated to the subsequent risk of infection. Here, we aim to develop a framework to quantify the relative risk of infection for different scenarios associated with the toilet plume using experimental measurements. The relative risk posed to a second susceptible individual using a toilet cubicle after faecal shedding and flush aerosolisation by an infected individual was evaluated as a case study for the methodology. This was carried out through a series of experimental measurements of particles released from a toilet flush, with the lid open, in a controlled chamber setting together with a mathematical modelling approach based on Quantitative Microbial Risk Assessment (QMRA) methods. The case study investigates how introducing the confined cubicle space and changing the ventilation rate affects relative risk, and also investigates the role played by different male and female toilet facility occupancy times. Findings are applicable to shared toilet facility settings such as hospitals, workplaces and social spaces, including public events (e.g. concerts, conferences, festivals).

2. Methods

2.1. Experimental methods

Experiments were performed in a mechanically ventilated chamber measuring $4.26 \times 3.35 \times 2.26 \text{ m}$. The air, filtered using a high-efficiency particulate air (HEPA) filter, was supplied through a high-level diffuser. Although HEPA filters are not common in toilet facilities, one was used here to eliminate the influence of particles external to the chamber on the particle concentration results. The air was extracted from a low-level diffuser positioned diagonally opposite to the inlet. Three ventilation rates were investigated: 1.5, 3 and 6 air changes per hour (ACH). These rates were selected based on guidance from the National Health Service (NHS) England which recommends 3 ACH for single room toilet facilities and 6 ACH for communal ward toilet facilities [37]. A rate of 1.5 ACH was then chosen to represent a poor ventilation scenario. The low-level outlet was set to a mass flow rate corresponding to the required ventilation rate and the high-level inlet was set so that the room operated at a negative pressure.

The toilet (Portland Close Coupled Toilet Pan, Cistern & Seat, Wickes) was typical of bathrooms in the United Kingdom, with a low-flow flush. The cistern had a maximum capacity of 6 L and was manually filled with water before each experiment. The toilet seat and lid were placed in the upright position. The toilet bowl was filled initially with 1 L of a 5 % NaCl solution in water. This created a safe aerosol, and salt solutions have previously been shown to behave in a similar way to microbial aerosols in air [38,39]. A flexible pipe was attached to the toilet waste pipe leading into a sealed bucket, allowing the wastewater to be collected after flushing and disposed of. To facilitate flushing, the toilet was mounted on a plinth to allow the wastewater to flow under gravity into the bucket, with a cable attached to the flushing mechanism. The cable led to the outside of the chamber so that it could be flushed remotely. Two optical particle counters (Handheld Particle Counter 3889, Kanomax) were used, supported by tripods, measuring particles with diameters of 0.3, 0.5, 1, 3, 5, and 10 μm . Temperature and relative humidity were monitored using an indoor air quality monitor (AirVisual Pro, IQAir).

Two scenarios were considered, described in Table I and illustrated in Fig. 1.

In scenario 2 (2 C), the cubicles were constructed using lab scaffolding and plastic sheet, with dimensions informed by British Standards [40]. However, it is important to note that cubicle design standards vary internationally. The particle counter locations and dimensions of the

Table I
Details of scenario 1 (NC) and scenario 2 (2 C) used for the experimental work.

Scenario	Abbreviation	Details	Particle counter locations
1	NC (no cubicle)	Toilet inside the chamber, against one wall.	A: directly above toilet, horizontally. B: next to the toilet, vertically.
2	2 C (two cubicles)	Toilet in the same location as scenario 1 (NC), but with the addition of two cubicles. One cubicle surrounded the toilet, the other was the same size and adjacent to the first cubicle.	A: inside toilet cubicle, directly above toilet, horizontally. B: inside toilet cubicle, next to the toilet, vertically.

cubicles can be seen in Fig. 2a) and b), respectively. A small gap existed below the cubicle of 0.11 m and a gap above the cubicle of 0.31 m.

Each experiment measured particle concentrations in the air during a single flush scenario. At the beginning of the experiment, the particle counters were set to run with a 10 s sample interval time, measuring the average concentration of particles over this period. The room was then vacated and left to ventilate at 11 ACH for 30 minutes, aimed at removing any particles generated during the process of entering the room and filling the toilet. The required ventilation rate for the experiment was set and left for 45 minutes, allowing the room to reach a steady state background level of particles. The toilet was flushed remotely from outside the room and, after 10 minutes, the particle counters were stopped. Experiments were performed in triplicate for each ventilation rate.

The experimental data were extracted from the particle counters and

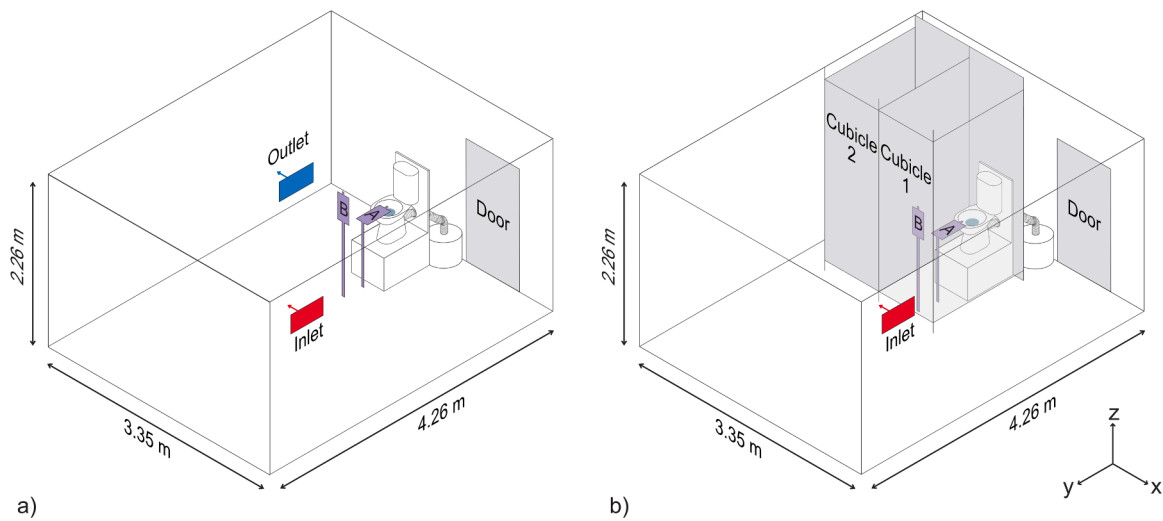


Fig. 1. The experimental arrangement for a) scenario 1 (NC) and b) scenario 2 (2 C).

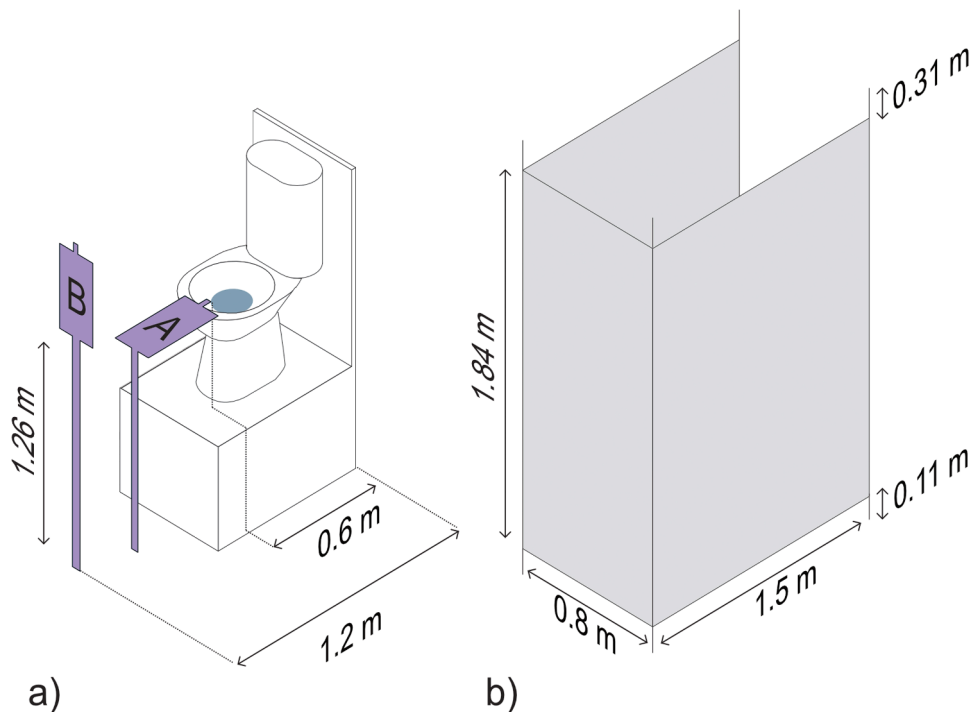


Fig. 2. a) Particle counter locations relative to the toilet mount and b) the dimensions of the toilet cubicle.

analysed using R (R version 4.3.2, run using RStudio 2023.12.0). A time series for the particle concentrations was generated by averaging the concentrations over the three replicate experiments. The standard error was included as a shaded range in plots, calculated from the standard deviation of experimental replicates.

2.2. Quantitative Microbial Risk Assessment (QMRA) model

Experimental data from scenarios 1 (NC) and 2 (2 C) at particle counter A were combined with published data on viral concentrations in faecal matter, toilet facility occupancy times, and understanding of aerosol physics to develop a QMRA model. This model was applied using data for two viruses, SARS-CoV-2, and norovirus. Specifically, it aimed to show how the framework could be used to compare the probability for a second individual becoming infected after entering the toilet facility following a flushing event by an infected individual, and to explore the behavioural and environmental factors that could affect this risk.

2.2.1. Gender-specific occupancy times

The infection risk was considered for both male and female cubicle occupancy times, t_{dur} [s], shown in Fig. 3, under various cubicle and ventilation scenarios observed in the experiments. The occupancy times used were from data in a shopping plaza during Autumn 1972 and Spring 1973 in Canada [41]. Although more recent empirical studies exist detailing bathroom occupancy times (a public bathroom study in 1988 [42], an airport bathroom study in 2016 [43] and a college study in 2009 [44]), these studies only detail the occupancy time of the bathroom as opposed to time spent in the cubicle. These studies include handwashing and drying, an act which varies between genders [45]. Another study of office buildings in 1976 only included the raw data for female cubicle occupancy times [46]. As we were interested in the time spent in the cubicle for both genders, as opposed to handwashing time, the data from the shopping plaza during Autumn 1972 and Spring 1973 was selected. Here, the model considered the second person entering the toilet facility immediately (0 s), 60 s and 240 s after the flush, using the appropriate particle concentration from the experimental data at this time. For each of the t_{enter} times, there were $N = 999$ (333 random values of t_{dur} sampled from Fig. 3 for each of the 3 replicates) simulations.

2.2.2. Uniformly distributed occupancy times

It was recognised that gender-specific bathroom behaviours measured in the Canadian study are a limited data set for a particular setting and period in time, with cubicle occupancy times potentially varying. To account for this, a sensitivity analysis was also performed. In

particular, the relationship between toilet facility occupancy time, t_{dur} [s], the time for a second individual to enter the toilet facility post-flush, t_{enter} [s], and corresponding normalised infection risk was investigated. For this part of the study, the cubicle occupancy time was sampled from a uniform distribution between [1, 900] s in a 1 s interval (i.e., 900 values). These occupancy times were simulated with, $t_{enter} \in [0, 599]$ s in a 1 s interval (i.e., 600 values). This corresponded to 540,000 (900 × 600) values of normalised infection risk. This investigation was therefore independent of the observational occupancy times in Fig. 3, with the sensitivity to all occupancy times studied instead.

2.2.3. Exposure modelling

The model framework used a stochastic Monte Carlo approach to calculate exposure by selecting parameters from realistic ranges and running multiple simulations to evaluate the range of risk. The number of particles inhaled by the second individual was first calculated and then the viral load of these particles was estimated to determine the likely exposure. Parameters and their distributions used for this QMRA model are detailed in Table II.

The concentrations of SARS-CoV-2 and norovirus in faecal matter, as shown in Table II, were derived from hospitalised cases. SARS-CoV-2 concentrations were based on samples collected on the first day of hospitalisation, while norovirus concentrations were based on samples from individuals hospitalised with gastroenteritis, with stool samples collected within 96 hours of symptom onset. Individuals at this stage of illness are unlikely to use shared public toilet facilities, which may lead to an overestimation of concentrations in this model. Those with mild symptoms who are not hospitalised are likely to shed lower concentrations of the viruses. For SARS-CoV-2, the peak concentration in faeces has been estimated to occur at 0.34 days post-symptom onset [58] while for norovirus, peak concentrations are observed within a few days of infection onset [59]. For both viruses, there is a large temporal variation in the concentration in faeces between people, which could result in either overestimation or underestimation of concentrations in the model.

For a given ventilation rate, particle size i , and experimental replicate j , the increase in concentration above background levels over time associated with flushing, $c_{i,j,t}$ [$\# / m^3$] was calculated as

$$c_{i,j,t} = c_{i,j,t}^{raw} - c_{i,j}^{background}, \quad (1)$$

where

$c_{i,j,t}^{raw}$ [$\# / m^3$] – average concentration returned by the particle counter over the 10 s sampling period and

$c_{i,j}^{background}$ [$\# / m^3$] – median measured particle concentration

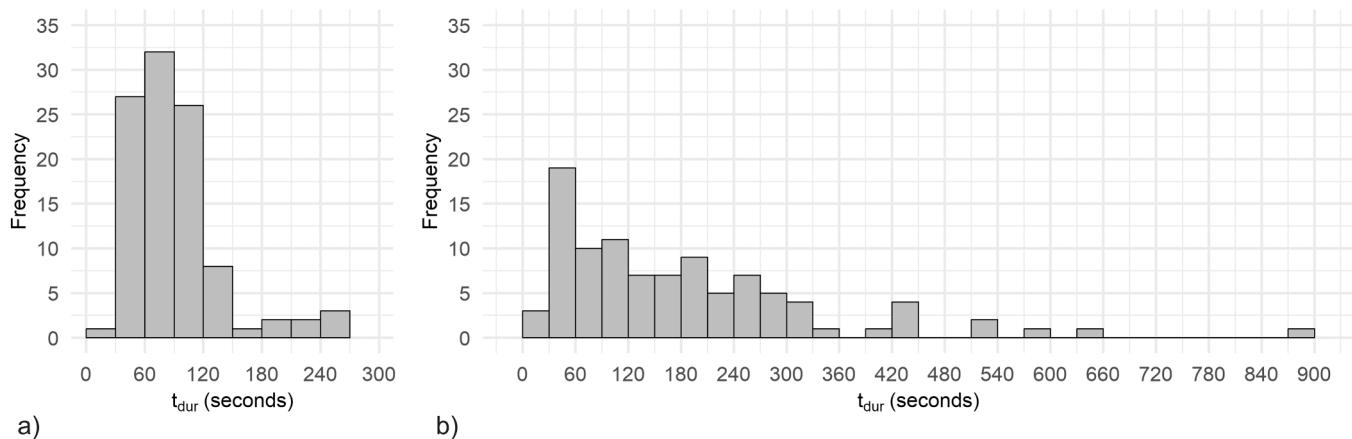


Fig. 3. Cubicle occupancy times for a) females and b) males for an enclosed mall-type suburban shopping plaza during Autumn of 1972 and Spring of 1973. Observations were made on Thursday and Friday evenings and during the day on Saturdays (i.e. the busiest times of the week). The figure has been generated based on observational data reported in [41].

Table II
Parameters used for the quantitative microbial risk assessment (QMRA) exposure model.

Parameter	Symbol	Unit	Distribution	Parameters	Source
Inhalation rate ¹	B	m^3 / s	Normal (truncated)	$\mu = 2.00 \times 10^{-4}$; $\sigma = 4.17 \times 10^{-5}$; min = 9.26×10^{-5} ; max = 2.69×10^{-4}	[47–49]
SARS-CoV-2 concentration in faeces	$\rho_{\text{SARS-CoV-2}}$	gc / L	Hockey-stick	min = 5.00×10^6 ; median = 1.3×10^8 ; max = 3.98×10^{10}	[50–53]
Norovirus concentration in faeces ²	$\rho_{\text{norovirus}}$	gc / L	Hockey-stick	min = 2.30×10^9 ; median = 9.02×10^{11} ; max = 6.10×10^{14}	[51,52,54,55]
Ratio of genome copies corresponding to infectious virus	f	gc / PFU	Uniform	min = 100; max = 1000	[56]
Volume of faecal matter ³	V_{faeces}	L	Normal (left-truncated at zero)	$\mu = 1.84 \times 10^{-1}$; $\sigma = 1.51 \times 10^{-1}$	[57]

¹ Men and women combined breathing rate for short exposure. Normal distribution assumed and standard deviation estimated by halve the difference of the 95th percentile and mean. Divided by 60 for volume per second.

² Density of faecal matter, $1.06 \times 10^3 \text{ g} / \text{L}$ multiplied by viral load per gram.

³ Mean diarrheal stool volume divided by number of stools for placebo group. Standard error propagated and standard deviation found using $n = 11$ placebo group participants.

across the 5 minutes prior to flushing.

If $c_{i,j,t}$ was returned as a negative value, it was set to zero. This analysis enabled the relative change in concentration over time, due to the flush, to be determined, while accounting for the background concentration measured before the flush.

For each experimental replicate j , the number of particles of size i , $i \in \{0.3, 0.5, 1, 3, 5, 10\} \mu\text{m}$, inhaled by a second susceptible individual, $N_{i,j}$, was estimated as

$$N_{i,j} = \int_{t_{\text{enter}}}^{t_{\text{enter}} + t_{\text{dur}}} c_{i,j,t} B dt, \quad (2)$$

where

B [m^3 / sec] – breathing rate.

In practice, Eq. (2) was implemented as a summation, as $c_{i,j,t}$ was a piecewise function.

In the experiments, it was assumed that particles measured just above the toilet after flushing had fully evaporated, possibly leading to a smaller measured diameter, d_i^{measured} which corresponded to an initial larger diameter, d_i when released. The model incorporated an initial droplet size derived from the measured droplet size, relative humidity, and the distance between the water in the bowl and the toilet surface. An approximation of the time dependent radius of an evaporating droplet [60], $R(t)$ [m], is given by

$$R(t) = \sqrt{R_0^2 - \theta(1 - \text{RH})t} \quad (3)$$

where

R_0 [m] – initial radius,

RH – relative humidity and

θ [$\text{m}^2 \text{s}^{-1}$] – 1.1×10^{-9} .

The speed of the droplet at the surface of the bowl, v_{surface} , was assumed to be $1 - 2 \text{ m} / \text{s}$ [36], and the distance between the water in the bowl and the surface of the bowl was measured to be 0.2 m . Using kinematics equations, with the droplet accelerating downwards due to gravity, the time for the droplets to reach the surface of the toilet bowl was assumed to be $0.083 - 0.124 \text{ s}$. The relative humidity in the room was assumed $40 - 50 \%$, based on experimental measurements. For each experiment, a relative humidity and v_{surface} was randomly sampled from a uniform distribution between 0.4 and 0.5 and $1 - 2 \text{ m} / \text{s}$ respectively. Table III summarises the maximum and minimum estimated initial droplet diameters using this method for each measured diameter.

The initial droplet size was then used to calculate the initial volume of droplets and hence the amount of virus that it potentially could carry

Table III

The estimated range of diameters of the initial droplet for each measured diameter using the extreme values for RH and v_{surface} .

Measured diameter (μm)	Estimated initial diameter range (μm)
0.3	13.5 – 18.1
0.5	13.5 – 18.1
1	13.5 – 18.1
3	13.9 – 18.4
5	14.4 – 18.8
10	16.8 – 20.7

before evaporation. The droplets were assumed to be spherical, with their volume, V_i^{droplet} [L], calculated as

$$V_i^{\text{droplet}} = \frac{\pi}{6} d_i^3 \times 1000. \quad (4)$$

The factor of 1000 accounted for the change of units (m^3 to L). To estimate the exposure dose, the droplet volume was used with data on virus in faecal matter and the results of $N_{i,j}$ from Eq. (2) to calculate the number of plaque forming units (PFU) carried by each droplet.

The dose in terms of genome copies for each replicate j , D_j^{gc} [gc], was equal to

$$D_j^{\text{gc}} = \sum_i N_{i,j} \times V_i^{\text{droplet}} \times \frac{V_{\text{faeces}}}{V_{\text{bowl}} + V_{\text{faeces}}} \times \frac{\rho_{\text{pathogen}}}{f}, \quad (5)$$

where

V_{faeces} [L] – volume of faecal matter per bowel movement,

V_{bowl} [L] – volume of water in the toilet bowl (1 L) and

ρ_{pathogen} [gc / L] – density of genome copies.

The corresponding dose in terms of infectious virus, D_j^{PFU} , was

$$D_j^{\text{PFU}} = \frac{D_j^{\text{gc}}}{f} \quad (6)$$

where

f [gc / PFU] – ratio of genome copies to infectious pathogen.

Eq. (5) assumes that the entire faecal matter was evenly distributed throughout the bowl, resulting in a consistent ratio of faecal matter to bowl water across the entire volume. This assumption might hold true for diarrhoea, which has a more liquid consistency, but solid matter would likely settle at the bottom of the bowl. Still, this assumption in Eq. (5) was based on a study where a toilet was flushed with *E. coli* in the bowl, and saw no appreciable difference in bacteria generation between flushing a solid stool and a homogenised stool [4]. It was also assumed

that the virus is uniformly distributed by volume within the initial droplet size. While studies have shown the potential for viral enrichment in certain aerosol sizes [10], there is no data available that would be appropriate to use in this scenario.

2.2.4. Dose-response model

A quantitative microbial dose-response relationship was then used to estimate the probability of infection for the second individual for a given dose. Such models are typically derived from human outbreak or animal data and are widely used for evaluating infection risks in air, water and food exposures [61]. For SARS-CoV-2, $P_{\text{infection}}(D^{\text{PFU}})$, an exponential model [62] was used such that

$$P_{\text{infection}}(D^{\text{PFU}}) = 1 - \exp(-k \times D^{\text{PFU}}), \quad (7)$$

where $k = 5.39 \times 10^{-2}$ [PFU⁻¹].

For norovirus, a Beta-Poisson model is more commonly applied [63, 64], and this was used such that

$$P_{\text{infection}}(D^{\text{gc}}) = 1 - \left(1 + \frac{\lambda \times D^{\text{gc}}}{\beta}\right)^{-\alpha}, \quad (8)$$

where $\alpha = 0.104$ and $\beta = 32.3$ [gc] are the fitted Beta-Poisson parameters. Unlike the SARS-CoV-2 dose-response model, the dose here is expressed in genome copies as opposed to PFU. A reduction factor, λ , is included in Eq. (8) to account for the assumption that particles are captured in the upper respiratory tract, subsequently removed by ciliary action, and passed to the digestive tract via the pharynx. A range of 10–50 % was applied for λ , informed by previous work [65]. This range was implemented using Monte Carlo simulations.

It was recognised that there was uncertainty in these estimates, both through the experimental measurements and the distributions selected for parameters. Infection risk was therefore calculated as a normalised infection risk, to allow comparison between scenarios.

For the gender-specific occupancy times (using the t_{dur} distributions in Fig. 3), a normalised infection risk was plotted as separate violin plot for $t_{\text{enter}} \in \{0, 60, 240\}$ s for each scenario and air change rate. The normalisation factor used was the maximum infection risk across both viruses, scenarios, ventilation rate and entry time. This allowed comparison of infection risk between the two virus types.

For the uniformly distributed occupancy times, a normalised infection risk as a function of both t_{enter} and t_{dur} was plotted as a heat map. The normalisation factor used was the median infection risk, $\tilde{P}_{\text{infection}}$, for each virus, across the two scenarios and ventilation rates. Bivariate Spearman rank correlation coefficients were used to assess the monotonic relationship between the parameters and the infection risk. This was implemented using the R package `cor()`. Correlation coefficients between infection risk and t_{enter} and t_{dur} respectively were calculated for two subsets of infection risk: i) $0 \text{ min} < t_{\text{enter}} \leq 1 \text{ min}$ and ii) 1 min

$< t_{\text{enter}} \leq 10 \text{ min}$. The strength of the correlation associated with the Spearman correlation coefficients is defined in Table IV.

3. Results and discussion

3.1. Particle concentration time-series

The mean measured particle concentrations (with the background concentration removed) for particle counter locations A and B are depicted in Figs. 4 and 5, respectively.

At particle counter location A, there was an initial rapid increase in particle concentrations across all particle sizes. This increase in concentration decayed to background levels as the particles released, due to the flush, were dispersed inside the room and were subsequently removed by ventilation. Following the initial decay, there were fluctuations in concentrations observed above zero particles per m³, which depicted variations in concentration around the background concentration. The time series was positively skewed due to concentrations below this background level being set to zero.

During the initial 10 seconds of flushing, larger concentrations were observed in scenario 1 (NC) compared to scenario 2 (2 C) for ventilation rates of 1.5 and 6 ACH. However, for 3 ACH, the concentrations were similar between scenarios. The variation in concentrations across different ventilation rates could be attributed to airflow patterns within the room, potentially leading to increased aerosolisation of particles in this specific region.

For particle counter location B, the initial spike in concentration was not observed. Although a spike occurred when close to the source for particle counter A, any increase at particle counter B remained below the limit of detection due to fluctuations in background levels. Thus, particles were dispersed within the room, resulting in a less noticeable increase. Because of this, a QMRA model was not performed using the data from particle counter B. For particles with diameters 3 and 5 μm , there was a small spike at 1 minute in Fig. 5a) and at 2.5 minutes in Fig. 5c). These increases in concentrations were again attributed to airflow patterns. These may be significant, as if an individual had been in the toilet facility during these specific times, they could inhale a large quantity of particles.





3.2. Quantitative Microbial Risk Assessment results

3.2.1. Gender-specific occupancy times

The normalised infection risk for the two scenarios for a susceptible individual entering the toilet facility after an individual infected with norovirus or SARS-CoV-2 flushed the toilet is illustrated in Fig. 6. Supplementary Table I gives the absolute mean and median infection risk values found for each of these scenarios for reference. The times indicated refer to the moment when the susceptible individual was exposed

Table IV

The strength of the correlation associated with the Spearman correlation coefficients.

Spearman correlation value, r_s	Strength of correlation relationship	Colour
$ r_s \geq 0.70$	Very strong	-
$0.40 \leq r_s < 0.70$	Strong	
$0.30 \leq r_s < 0.40$	Moderate	
$0.20 \leq r_s < 0.30$	Weak	
$ r_s < 0.20$	Negligible	

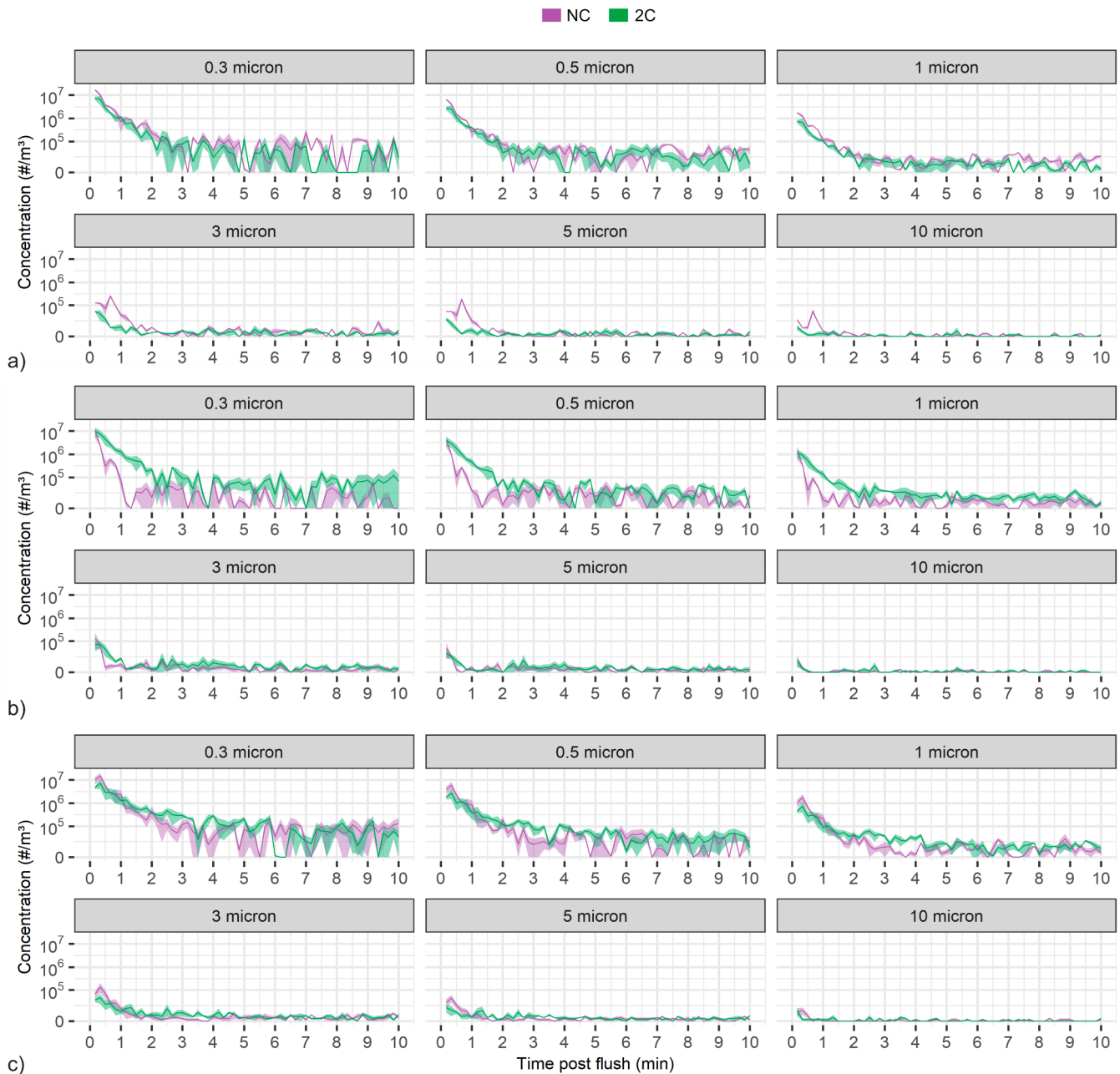


Fig. 4. Particle concentrations at location A of the particle counter, with the background concentration removed (median concentration 5 minutes before flushing), during the 10 minutes post-flush for a) 1.5 ACH, b) 3 ACH, and c) 6 ACH. Shaded areas denote standard error across replicates.

to the aerosols after the toilet had been flushed, t_{enter} . This will be used as the time at which the second individual enters the toilet facility. It is worth noting that zero seconds may be considered as an unrealistic entry time but was provided for comparison purposes.

Across the two scenarios, virus types and $t_{\text{enter}} = \{0, 60, 240\}$ s, the estimated absolute infection risk ranged from $1.4 \times 10^{-7}\%$ to 73.6%. These minimum and maximum values represent extreme cases, with the low density indicating their lower likelihood. High risk values correspond to the highest inhaled doses, which, as per Eqs. (2) and (5), depended on various factors such as time spent in the toilet facility and breathing rate. There may be an overestimation in the stated infection risks, as any positive variation above the background concentration in the experimental data was considered to contain infectious particles. In reality, these non-zero concentrations may have stemmed from positive fluctuations in background levels around the background count rather than particles that have originated from the flush. This was especially

true for smaller-sized particles, which exhibited greater fluctuations in background concentration in absolute terms.

The normalised risk linked with exposure to norovirus was larger with the maximum infection risk 2 times greater for norovirus than the maximum infection risk for SARS-CoV-2. This was due to the difference in measured viral concentration of the pathogens in faeces used as a data input to the model [50,53–55] (see Table II) and the difference in the dose response model [62–64] (see Eqs. (7) and (8)). We acknowledge however, that knowledge of both viral load in faecal matter and the infectious dose for SARS-CoV-2 was more limited than for norovirus and therefore there was uncertainty in these estimates.

There were differences between male and female normalised infection risk in all scenarios. Recall, the difference in male and female occupancy times shown in Fig. 3 was based on observational data. The mean occupancy times in the model were 173 s for men and 95 s for women. In Fig. 6, for a given scenario, the normalised mean risk of

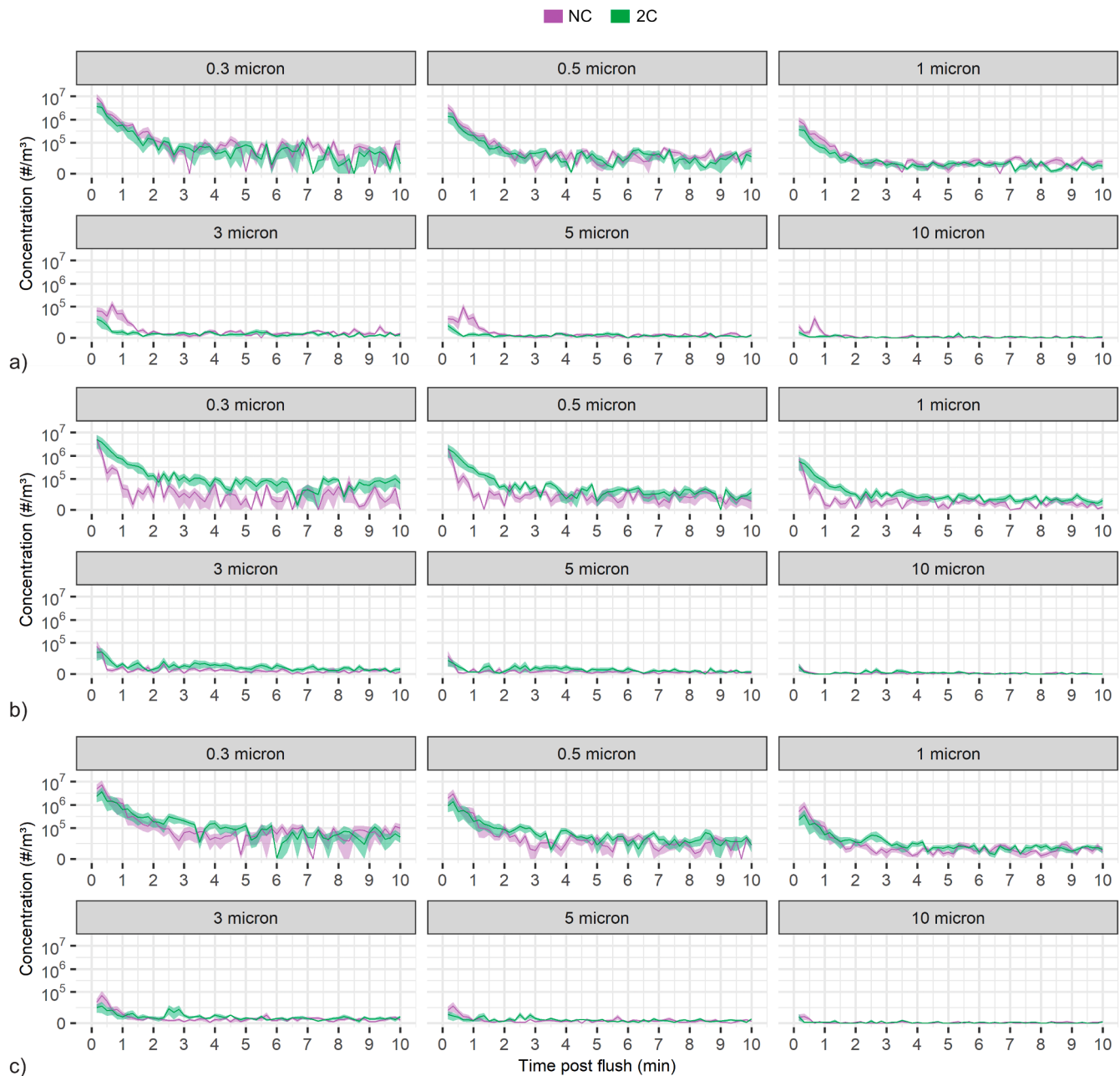


Fig. 5. Particle concentrations at location B of the particle counter, with the background concentration removed (median concentration 5 minutes before flushing), during the 10 minutes post-flush for a) 1.5 ACH, b) 3 ACH, and c) 6 ACH. Shaded areas denote standard error across replicates.

infection decreased as the time to enter the cubicle after flushing increased. For example, in the 1.5 ACH cubicle scenario (2 C) with norovirus as the modelled virus (Fig. 6b) the normalised mean infection risk across both genders saw a decrease of 41.03% between $t_{\text{enter}} = 0$ and 60 s and an 66.7% decrease between $t_{\text{enter}} = 0$ and 240 s. For the same scenario using SARS-CoV-2 as the modelled virus (Fig. 6a), the normalised mean infection risk saw a decrease of 85.0% between $t_{\text{enter}} = 0$ and 60 s and a 94.6% decrease between $t_{\text{enter}} = 0$ and 240 s. This indicated that allowing removal of aerosol by ventilation and deposition after flushing is likely to be crucial in reducing the risk of infection. Among the 36 cases depicted in Figs. 6, 72.2% (26/36) showed a higher normalised mean infection risk for men. However, the empirical data on toilet facility occupancy times across genders, originating from a suburban shopping plaza in Canada, may not directly apply to other settings, for example hospitals, public events or workplaces. Gathering additional behavioural data specific to individual scenarios and different

groups of people is necessary for a better understanding of exposure risks.

For both viruses, at 3 ACH and for $t_{\text{enter}} = 0, 60$ and 240 s, there was a greater estimated normalised mean infection risk for scenario 2 (2 C), compared to scenario 1 (NC). At 6 ACH, $t_{\text{enter}} = 60$ and 240 s showed the same trend, but $t_{\text{enter}} = 0$ s had a greater normalised mean infection risk for scenario 1 (NC). In these cases, the presence of a cubicle may potentially entrain more particles inside the cubicle, resulting in exposure to a higher dose. At 1.5 ACH, scenario 2 (2 C) showed a lower mean risk of infection in all cases. Again, airflow patterns are significant here to understand the trajectory of these droplets.

The difference between male and female normalised mean infection risks was smaller in comparison to the effect of other variables, such as t_{enter} . This may be due to the fact that the release of particles was seen to be a highly transient process and most particles were detected as a spike in the first 2 minutes as discussed in Section 3.1.

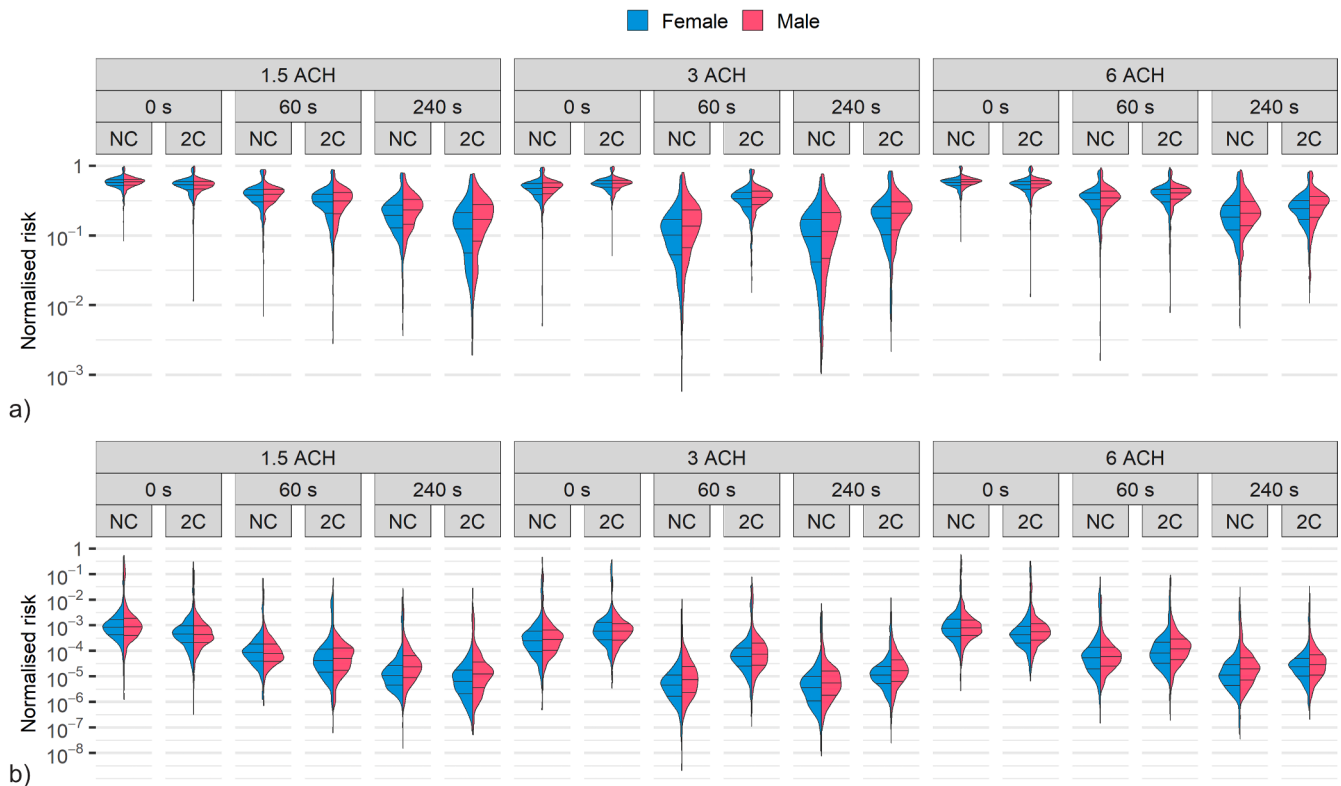


Fig. 6. Violin plots corresponding to the normalised risk associated with a) norovirus and b) SARS-CoV-2 for particle counter A. Infection risk was normalised by the maximum value across all virus, scenario and ventilation rates (this was obtained for norovirus, NC, $t_{\text{enter}} = 0$ s, 1.5 ACH). The times referred to indicate the moment when the susceptible individual entered post-flush, t_{enter} . NC and 2C refer to scenarios as described in Table I. Horizontal lines represent the 25th, 50th, and 75th quantiles.

3.2.2. Uniformly distributed occupancy times

Figs. 7 and 8 show how normalised SARS-CoV-2 and norovirus infection risk varied with t_{enter} and t_{dur} respectively. The normalised infection risk still retained a stochastic element due to the random selection of the dose from the experimental replicates.

The red regions, indicating higher infection risk, are concentrated in areas where the entry time (t_{enter}) was less than 60 s, and in some cases, even less than 30 s. This zone exhibited the highest relative risks. Even with shorter occupancy times, the risk remained significantly higher compared to areas where t_{enter} exceeded a minute. Therefore, to mitigate risk more effectively, it may be more advantageous to increase t_{enter} rather than solely reducing occupancy time. We recommend waiting at least 60 s before entering the toilet facility, based on a comparison of the normalised infection risks in the region $t_{\text{enter}} < 1$ min and $1 \text{ min} \leq t_{\text{enter}} < 10$ min. For norovirus in scenario 1 (NC), 78.6 % of the normalised infection risks exceeded the norovirus median infection risk when $t_{\text{enter}} < 1$ min and for scenario 2 (2C), this was 89.0 %. In the region $1 \text{ min} \leq t_{\text{enter}} < 10$ min, 46.8 % and 52.9 % of the risks exceeded the median infection risk for scenarios 1 (NC) and 2 (2C), respectively. For SARS-CoV-2, 78.9 % of the normalised infection risks exceeded the SARS-CoV-2 median infection risk in scenario 1 (NC) when $t_{\text{enter}} < 1$ min and 89.0 % in scenario 2 (2C). In contrast, 46.8 % and 53.2 % exceed the median risk when $1 \text{ min} \leq t_{\text{enter}} < 10$ min in scenarios 1 (NC) and 2 (2C), respectively. Thus, increasing t_{enter} significantly reduced the likelihood of having a higher infection risk. Providing sufficient toilet facilities and cubicles can help minimise the need to enter immediately after someone has flushed, helping to mitigate the risk of infection from the close exposure to the toilet plume. However, providing additional cubicles and toilet facilities incurs economic costs related to construction, planning, and the increased space requirements for accommodating more facilities.

The values of the Spearman correlation coefficients for SARS-CoV-2 and norovirus, calculated using the R package `cor()`, can be seen in Tables V and VI respectively. The associated strength of the correlation was described previously in Table IV. This analysis is used to explore the relative importance of different parameters in the model.

For the narrower range of $0 \text{ min} < t_{\text{enter}} \leq 1$ min, the relationship between infection risk and occupancy time (t_{dur}) was negligible to weak, as infection risk during this period was primarily driven by t_{enter} . The relationship between infection risk and the time the second individual entered the toilet facility (t_{enter}) was strong, with one moderate case, within this 0 min to 1 min window. For $1 \text{ min} < t_{\text{enter}} \leq 10$ min, the influence of t_{enter} on infection risk was negligible or, in two cases, moderate, whereas the relationship with occupancy time (t_{dur}) was strong, or in one case moderate. This suggests that if the second individual enters the toilet facility within the first 1 minute after flushing, the infection risk is heavily dependent on the time which they enter. Specifically, the negative relationship shows that the risk decreases as the delay in entry increases. During this early period, the risk was less dependent on how long they occupied the cubicle, indicating that reducing occupancy time would have minimal impact on reducing infection risk in this region. Conversely, if the second individual enters after the first 1 minute, the infection risk becomes strongly dependent on how long they remain in the toilet facility.

The relationship between infection risk and factors such as i) breathing rate, ii) relative humidity, and iii) the velocity of droplets at the toilet surface was negligible within the model. However, the volume of faecal matter (V_{faeces}) showed a moderate to strong correlation with infection risk. The density of genome copies per litre of faecal matter (ρ), the ratio of genome copies corresponding to infectious virus (f) and the reduction factor λ , had a moderate to strong relationship, a moderate relationship and a weak relationship to infection risk respectively.

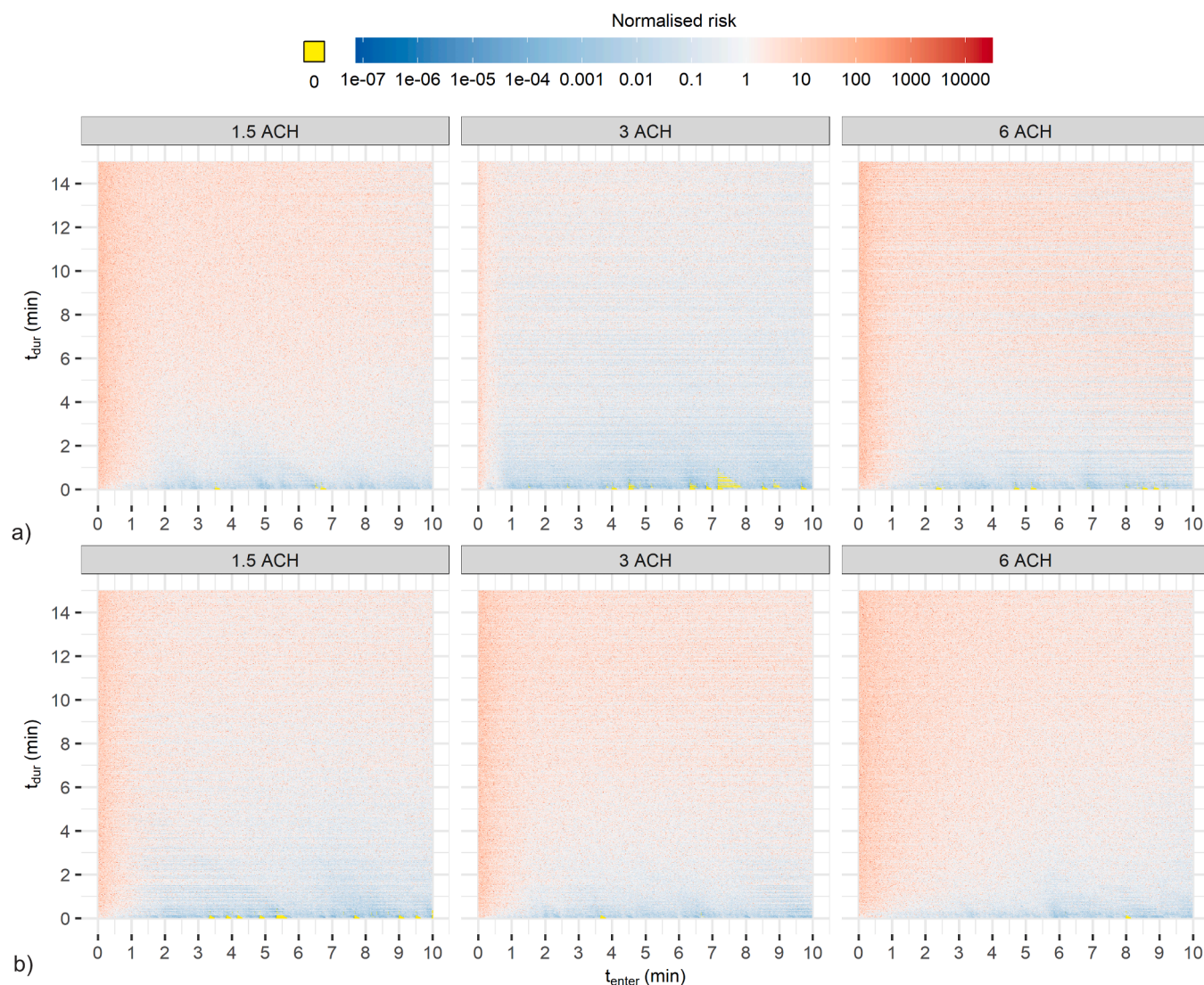


Fig. 7. Heat maps for a) scenario 1 (NC) and b) scenario 2 (2 C) showing the relationship between t_{enter} , t_{dur} and normalised SARS-CoV-2 risk infection. The particle counter was at location A and infection risk was normalised by the median value across the two scenarios and air change rates for SARS-CoV-2, $\bar{P}_{infection} = 2.6 \times 10^{-5}\%$.

Given the data from the literature, these findings suggest that further research should focus on collecting data on the volume of faecal matter per bowel movement and the density of genome copies per litre of faecal matter, as these factors have the most significant impact on estimated infection risks.

3.3. Implications and limitations

This study primarily addresses the development of an approach for the quantification of airborne transmission risks from the toilet plume and the application to two viruses illustrates a risk that is likely to have considerable variation, but that cannot be considered negligible. Mitigations to reduce airborne exposures, such as ensuring effective ventilation and managing use of shared toilet facilities, particularly by people who are known to be infectious or are particularly vulnerable, are important. We only consider inhalation exposure, at a specific close distance to the toilet but in real-life situations, droplets will also settle on surfaces within the toilet environment. This could potentially lead to fomite transmission when individuals come into contact with surfaces such as door handles or toilet paper holders [66]. Such transmission routes are particularly significant for faecal-oral diseases like norovirus.

In the case of respiratory diseases such as COVID-19, the exhalation of an infected individual into the cubicle could also release infectious virus, potentially resulting in a higher contamination than released from a discrete flush for some people.

Bacteria have been shown to be released during subsequent toilet flushes, though in decreasing numbers [1,67]. This suggests that the risk may extend beyond the first susceptible individual exposed after an infected individual, as residual pathogens in the bowl could still pose a hazard, albeit at lower concentrations. If multiple infected individuals use the same toilet throughout the day, the bowl could become consistently contaminated, increasing the likelihood of exposure and infection for all susceptible individuals using the facility. The possible pre-contamination of the toilet bowl is not something that was considered here and could be included in further modelling.

After calculating the pathogen load of droplets, the distinction of droplet sizes was disregarded, and the stages of the respiratory tract were also not accounted for. Different sized particles, which vary between the toilet plume and exhaled breath, are deposited at different parts of the respiratory tract. For the same number of virions, a difference in droplet size can impact infection risk and severity of illness depending upon where the particle was deposited. The locations of the

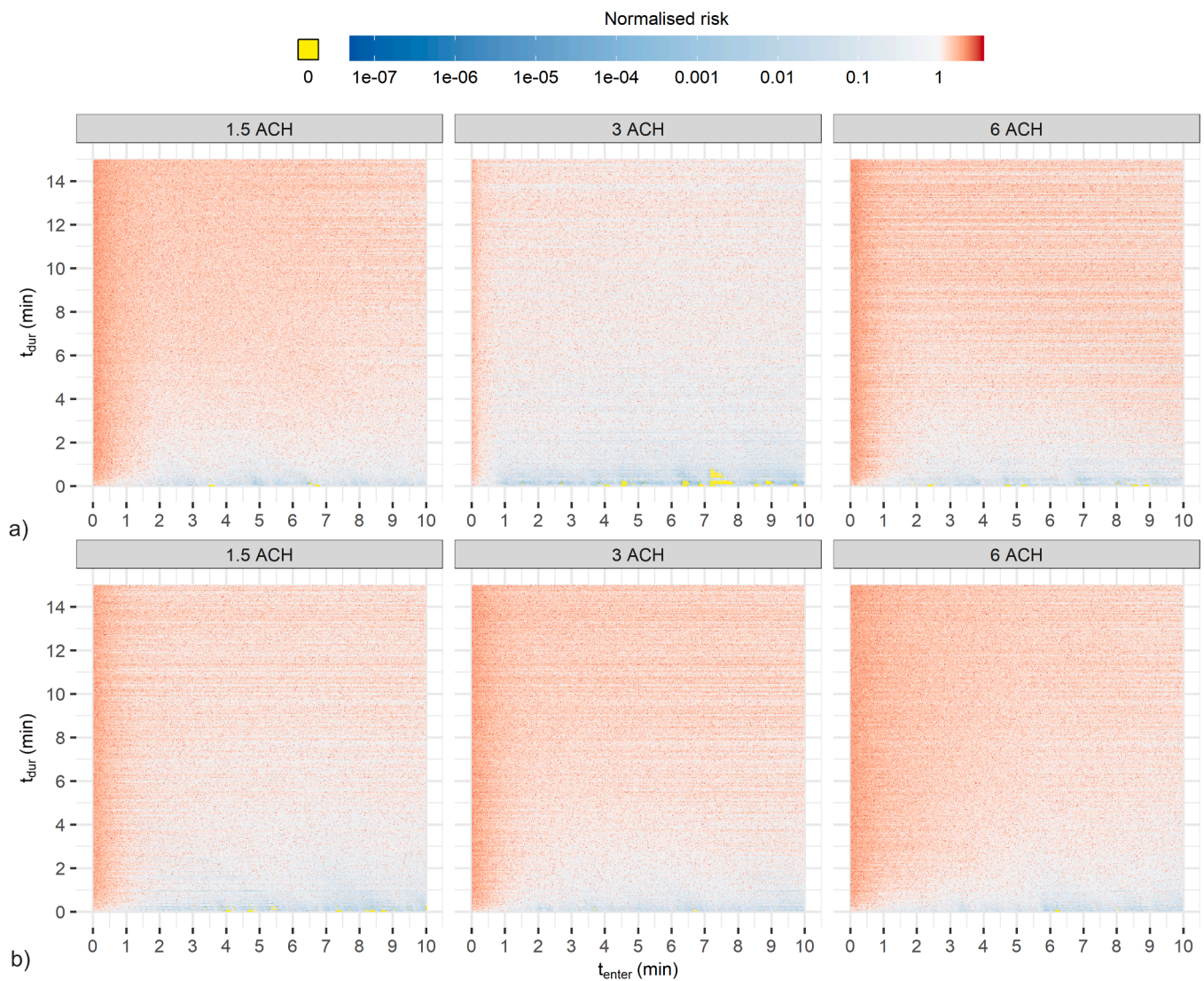


Fig. 8. Heat maps for a) scenario 1 (NC) and b) scenario 2 (2 C) showing the relationship between t_{enter} , t_{dur} and normalised norovirus risk infection. The particle counter was at location A and infection risk was normalised by the median value across the two scenarios and air change rates for norovirus, $\bar{P}_{\text{infection}} = 21.5\%$.

virus receptors also have an impact on whether deposition in the respiratory tract will initiate infection at all and if so the severity of the illness [68]. Dose-response models considering the probability of infection at different regions of the respiratory tract (upper vs lower) have been developed [69,70] and the Multiple-Path Particle Dosimetry Model (MPPD) can be used to model deposition in the respiratory tract [71]. This could be used in future work to adapt the model. In addition to this, the viral load was unlikely to be distributed proportionally to the volume as we have assumed. The virus distribution across droplet sizes will vary between exhaled breath and the toilet plume.

The transmission of norovirus via aerosolisation has been discussed in recent work [72] with more cases associated with vomiting, as opposed to diarrhoea. One suggestion of the study was the need for further research to investigate the role of diarrhoea and toilet flushing in the transmission of aerosols. Such research would contribute to this study and the applicability of norovirus as a chosen pathogen. We also modelled the exposure via inhalation with a reduction factor to account for ingestion. Respiratory activities are likely to play a part in ingestion, as particles deposited in the upper parts of the respiratory system may be ingested via mucus and saliva in the mouth, nose and throat. The actual mechanism for exposure to norovirus in the air will be much more complex than we are able to consider here, which could mean that the

infection risks modelled may be an overestimate or underestimate. As knowledge of exposure routes for pathogens increase, models such as that presented here can be refined to incorporate more complex exposure mechanisms. Recent modelling has determined where viruses predominantly deposit after inhalation, showing, for instance, that SARS-CoV-2 primarily deposits in the nasal region [68]. A similar approach could be applied to norovirus to estimate the proportion of inhaled virus depositing in the nasal region and subsequently ingested. This would refine the current study's assumption of a uniform 10–50% reduction factor

As discussed, a normalised risk was calculated to allow for comparisons of relative risks. Further work may focus on calibrating the model with data on virus concentrations produced from flushing the toilet and including factors such as the ratio of solid faeces to water. This would likely give more reliable absolute infection risk values. Such studies are essential but are challenging to carry out as they would require extensive experimental bioaerosol sampling using controlled seeding of a toilet under different realistic stool-water scenarios. These types of samples are difficult to obtain, as the transient nature of the flush and subsequent plume mean that the time evolution of viral particles in air happens quicker than the sample time for current bioaerosol sampling techniques. Similarly, the dose-response models carry some uncertainty as

Table V

Spearman correlation coefficients, r_s , between respective parameters and SARS-CoV-2 infection risk.

Parameter	t_{enter} (min)	Scenario 1 (NC)			Scenario 2 (2C)		
		1.5 ACH	3 ACH	6 ACH	1.5 ACH	3 ACH	6 ACH
t_{dur}	0 – 1	0.17	0.22	0.15	0.15	0.17	0.18
	1 – 10	0.43	0.42	0.40	0.45	0.45	0.40
t_{enter}	0 – 1	-0.40	-0.46	-0.44	-0.39	-0.37	-0.30
	1 – 10	-0.15	-0.11	-0.08	-0.13	-0.13	-0.28
f	0 – 10	-0.36	-0.32	-0.30	-0.32	-0.34	-0.34
ρ	0 – 10	0.39	0.37	0.34	0.36	0.38	0.39
B	0 – 10	0.12	0.11	0.10	0.11	0.11	0.11
V_{faeces}	0 – 10	0.40	0.37	0.33	0.37	0.38	0.39
RH	0 – 10	-0.05	-0.04	-0.04	-0.04	-0.05	-0.05
v_{surface}	0 – 10	-0.11	-0.10	-0.09	-0.10	-0.10	-0.11

Table VI

Spearman correlation coefficients, r_s , between respective parameters and norovirus infection risk.

Parameter	t_{enter} (min)	Scenario 1 (NC)			Scenario 2 (2C)		
		1.5 ACH	3 ACH	6 ACH	1.5 ACH	3 ACH	6 ACH
t_{dur}	0 – 1	0.17	0.22	0.15	0.16	0.18	0.19
	1 – 10	0.45	0.41	0.39	0.47	0.47	0.41
t_{enter}	0 – 1	-0.42	-0.46	-0.46	-0.40	-0.39	-0.30
	1 – 10	-0.16	-0.12	-0.08	-0.13	-0.13	-0.29
λ	0 – 10	-0.27	-0.25	-0.22	-0.24	-0.26	-0.27
ρ	0 – 10	0.42	0.39	0.37	0.39	0.40	0.41
B	0 – 10	0.12	0.11	0.10	0.11	0.12	0.12
V_{faeces}	0 – 10	0.41	0.37	0.34	0.37	0.39	0.39
RH	0 – 10	-0.05	-0.05	-0.04	-0.04	-0.05	-0.05
v_{surface}	0 – 10	-0.11	-0.10	-0.09	-0.10	-0.10	-0.10

there is a lack of good data on infection risks for different exposure routes for many pathogens.

The model uses normalised risk values to compare infection risks

across scenarios and pathogen types. With further calibration, it could provide more specific guidance on t_{enter} based on the infectious dose of the pathogen. This would be particularly beneficial when the infector

and pathogen type are known, especially if the susceptible individual has vulnerabilities. In cases where the infectious dose for a pathogen is particularly high, the maximum infection risk from the toilet plume may be negligible, and further efforts to reduce the infection risk may not be necessary.

The toilet occupancy times used were derived from a study in 1972. We recognise that there may be changes in human behaviour since 1972 and the present day, such as smartphone use in a toilet facility which could increase the time spent in a toilet cubicle [73]. Further behavioural data is needed to accurately describe contemporary cubicle occupancy. This could involve mock observational studies, though this may give an inaccurate representation of actual behaviour. Alternatively, using automatic sensors on cubicle doors could provide more accurate, real-world measurements.

This study examines an idealised scenario featuring mechanical ventilation and considers only two specific arrangements of the toilet facility. It is worth noting that ventilation systems may not operate perfectly, and the layout of each toilet facility may differ from those analysed in this study. Toilet facilities typically do not use HEPA filters, as were used in this study, which may result in exposure to external contaminants. Further investigation using CFD analyses is planned to better discern the effects of airflow patterns within particular ventilation systems and how the cubicle influences this. This would provide insight into how these airflow dynamics affect the trajectory of droplets and aerosols released from the toilet plume.

4. Conclusion

This study presents a new quantitative framework for estimating the potential for infection risk following a toilet flush and exposure to viruses released in aerosol. The model is applied for two viruses, and several ventilation and occupancy scenarios, based on particle data from controlled chamber experiments. The QMRA framework can in future be applied to other experimental particle measurements looking at different scenarios, for example alternative bathroom arrangements, or studying the toilet lid closed as opposed to open. The results enable the following conclusions to be drawn:

- The combined experimental and QMRA approach suggests that the infection risk from the toilet plume is highly variable but can be non-negligible. This may particularly be the case for certain pathogens, which have higher concentrations in faecal matter such as norovirus.
- The model framework allows exploration of factors that influence risk, and mitigating measures. Results suggest that when entering the toilet facility after an individual, it is important to allow the room to ventilate. Even waiting 60 s between occupants can decrease the risk of infection significantly.
- When considering adjustments to occupancy time (t_{dur}) and time between toilet facility use after another individual has flushed (t_{enter}), to mitigate risk we propose increasing t_{enter} to a minimum of 60 s as a more effective strategy compared to reducing occupancy time.
- Improved quantitative data is necessary to enhance the accuracy of the results and enable absolute risks to be determined. This includes toilet cubicle occupancy times especially concerning individual scenarios (e.g. hospitals, workplaces and public events), as well as data on virus concentrations in faeces, particle generation rates from different toilets and dose-response for different pathogens.

Funding sources

C A Higham is funded by the Engineering and Physical Sciences Research Council (EPSRC) Centre for Doctoral Training (CDT) in Fluid Dynamics [Grant Number EP/S022732/1].

CRedit authorship contribution statement

Catherine J. Noakes: Methodology, Writing – review & editing, Supervision, Funding acquisition, Conceptualization. **Martín López-García:** Writing – review & editing, Supervision, Methodology, Funding acquisition, Conceptualization. **Ciara Angel Higham:** Writing – review & editing, Writing – original draft, Visualization, Validation, Software, Project administration, Methodology, Investigation, Funding acquisition, Formal analysis, Data curation, Conceptualization. **Louise Fletcher:** Writing – review & editing, Supervision, Methodology, Funding acquisition, Conceptualization. **Emma Tidswell:** Resources, Methodology.

Declaration of Competing Interest

The authors declare the following financial interests/personal relationships which may be considered as potential competing interests: During the COVID-19 pandemic Prof. C J Noakes was a participant in the UK Scientific Advisory Group for Emergencies (SAGE) and co-chaired the SAGE Environment and Modelling Sub-Group. If there are other authors, they declare that they have no known competing financial interests or personal relationships that could have appeared to influence the work reported in this paper.

Acknowledgements

All authors would like to acknowledge the support of the late Phil Dolan whose keen interest and enthusiasm into our research will be dearly missed. The authors extend their gratitude to Dr David Elliott, Morgan McGowan, and Karen Stevens for their support in the experimental work conducted for this paper.

Appendix A. Supporting information

Supplementary data associated with this article can be found in the online version at [doi:10.1016/j.indenv.2024.100069](https://doi.org/10.1016/j.indenv.2024.100069).

Data Availability

The data and code required to produce the work can be found at https://github.com/ciarahigham/QMRA_toilet_plume

References

- [1] J. Barker, M.V. Jones, The potential spread of infection caused by aerosol contamination of surfaces after flushing a domestic toilet, *J. Appl. Microbiol.* 99 (2005) 339–347, <https://doi.org/10.1111/j.1365-2672.2005.02610.x>.
- [2] H.M. Darlow, W.R. Bale, Infective Hazards of Water-closets, *Lancet* 273 (1959) 1196–1200, [https://doi.org/10.1016/S0140-6736\(59\)91201-2](https://doi.org/10.1016/S0140-6736(59)91201-2).
- [3] D.L. Johnson, K.R. Mead, R.A. Lynch, D.V.L. Hirst, Lifting the lid on toilet plume aerosol: a literature review with suggestions for future research, *Am. J. Infect. Control* 41 (2013) 254–258, <https://doi.org/10.1016/j.ajic.2012.04.330>.
- [4] C.P. Gerba, C. Wallis, J.L. Melnick, Microbiological hazards of household toilets: droplet production and the fate of residual organisms, *Appl. Microbiol.* 30 (1975) 229–237.
- [5] D. Johnson, R. Lynch, C. Marshall, K. Mead, D. Hirst, Aerosol generation by modern flush toilets, *Aerosol Sci. Technol.* 47 (2013) 1047–1057, <https://doi.org/10.1080/02786826.2013.814911>.
- [6] European Centre, for, Disease Prevention, Control, C. Suetens, T. Kärki, D. Plachouras, Point Prevalence Survey of Healthcare-associated Infections and Antimicrobial Use in European Acute Care Hospitals – 2016–2017, *European Centre for Disease Prevention and Control*, 2023.
- [7] E.L. Best, J.A.T. Sandoe, M.H. Wilcox, Potential for aerosolization of *Clostridium difficile* after flushing toilets: the role of toilet lids in reducing environmental contamination risk, *J. Hosp. Infect.* 80 (2012) 1–5, <https://doi.org/10.1016/j.jhin.2011.08.010>.
- [8] M.P. Goforth, S.A. Boone, J. Clark, P.B. Valenzuela, J. McKinney, M.K. Ijaz, et al., Impacts of lid closure during toilet flushing and of toilet bowl cleaning on viral contamination of surfaces in United States restrooms, *Am. J. Infect. Control* 52 (2024) 141–146, <https://doi.org/10.1016/j.ajic.2023.11.020>.

- [9] W.F. Wells, On Air-borne Infection Study II. Droplets and droplet nuclei, *Am. J. Epidemiol.* 20 (1934) 611–618, <https://doi.org/10.1093/oxfordjournals.aje.a118097>.
- [10] C.C. Wang, K.A. Prather, J. Sznitman, J.L. Jimenez, S.S. Lakdawala, Z. Tufekci, et al., Airborne transmission of respiratory viruses, *Science* 373 (2021) eabd9149, <https://doi.org/10.1126/science.abd9149>.
- [11] W. Chen, N. Zhang, J. Wei, H.-L. Yen, Y. Li, Short-range airborne route dominates exposure of respiratory infection during close contact, *Build. Environ.* 176 (2020) 106859, <https://doi.org/10.1016/j.buildenv.2020.106859>.
- [12] J. Jung, J. Lee, S. Jo, S. Bae, J.Y. Kim, H.H. Cha, et al., Nosocomial outbreak of COVID-19 in a Hematologic Ward, *Infect. Chemother.* 53 (2021) 332–341, <https://doi.org/10.3947/ic.2021.0046>.
- [13] K.R. McKinney, Y.Y. Gong, T.G. Lewis, Environmental transmission of SARS at Amoy Gardens, *J. Environ. Health* 68 (2006) 26–30, quiz 51–2.
- [14] M. Kang, J. Wei, J. Yuan, J. Guo, Y. Zhang, J. Hang, et al., Probable evidence of fecal aerosol transmission of SARS-CoV-2 in a high-rise building, *Ann. Intern. Med.* 173 (2020) 974–980, <https://doi.org/10.7326/M20-0928>.
- [15] M.-A. Widdowson, R. Glass, S. Monroe, R.S. Beard, J.W. Bateman, P. Lurie, et al., Probable transmission of norovirus on an airplane, *JAMA* 293 (2005) 1859–1860, <https://doi.org/10.1001/jama.293.15.1859>.
- [16] M.S. Ho, R.I. Glass, S.S. Monroe, H.P. Madore, S. Stine, P.F. Pinsky, et al., Viral gastroenteritis aboard a cruise ship, *Lancet* 2 (1989) 961–965, [https://doi.org/10.1016/S0140-6736\(89\)90964-1](https://doi.org/10.1016/S0140-6736(89)90964-1).
- [17] Z.J. Madewell, Y. Yang, Ira M. Longini, J. Halloran, M.E. Dean, NE. Household secondary attack rates of SARS-CoV-2 by variant and vaccination status: an updated systematic review and meta-analysis, *JAMA Netw. Open* 5 (2022) e229317, <https://doi.org/10.1001/jamanetworkopen.2022.9317>.
- [18] N. Derqui, A. Koycheva, J. Zhou, T.D. Pillay, M.A. Crone, S. Hakkii, et al., Risk factors and vectors for SARS-CoV-2 household transmission: a prospective, longitudinal cohort study, *Lancet Microbe* 4 (2023) e397–e408, [https://doi.org/10.1016/S2666-5247\(23\)00069-1](https://doi.org/10.1016/S2666-5247(23)00069-1).
- [19] Z.A. Marsh, S.P. Grytdal, J.C. Beggs, E. Leshem, P.A. Gastañaduy, B. Rha, et al., The unwelcome houseguest: secondary household transmission of norovirus, *Epidemiol. Infect.* 146 (2017) 159, <https://doi.org/10.1017/S0950268817002783>.
- [20] N.A. Vielot, O. Zepeda, Y. Reyes, F. González, C. Toval-Ruiz, N. Munguia, et al., Transmission patterns of norovirus from infected children to household members in León, Nicaragua, *J. Pediatr. Infect. Dis. Soc.* 13 (2024) 148–151, <https://doi.org/10.1093/jpids/piad114>.
- [21] L.A. Paul, N. Daneman, K.A. Brown, J. Johnson, T. van Ingen, E. Joh, et al., Characteristics associated with household transmission of severe acute respiratory syndrome Coronavirus 2 (SARS-CoV-2) in Ontario, Canada: a cohort study, *Clin. Infect. Dis.* 73 (2021) 1840–1848, <https://doi.org/10.1093/cid/ciab186>.
- [22] M.B. Termansen, S. Frische, Fecal-oral transmission of SARS-CoV-2: a systematic review of evidence from epidemiological and experimental studies, *Am. J. Infect. Control* 51 (2023) 1430–1437, <https://doi.org/10.1016/j.ajic.2023.04.170>.
- [23] S. Barroso-Arévalo, B. Rivera, L. Domínguez, J.M. Sánchez-Vizcaíno, First detection of SARS-CoV-2 B.1.1.7 variant of concern in an asymptomatic dog in Spain, *Viruses* 13 (2021) 1379, <https://doi.org/10.3390/v13071379>.
- [24] Gortázar, C. Barroso-Arévalo, S. Ferreras-Colino, E. Isla, J. Fuente, G. de la, B. Rivera, et al., Natural SARS-CoV-2 infection in kept ferrets, Spain, *Emerg. Infect. Dis.* 27 (2021) 1994, <https://doi.org/10.3201/eid2707.210096>.
- [25] J. Dergham, J. Delerce, M. Bedotto, B. La Scola, V. Moal, Isolation of viable SARS-CoV-2 Virus from Feces of an immunocompromised patient suggesting a possible fecal mode of transmission, *J. Clin. Med.* 10 (2021) 2696, <https://doi.org/10.3390/jcm10122696>.
- [26] U. Das Adhikari, G. Eng, M. Farcasanu, L.E. Avena, M.C. Choudhary, V.A. Triant, et al., Fecal severe acute respiratory Syndrome Coronavirus 2 (SARS-Cov-2) RNA is associated with decreased Coronavirus Disease 2019 (COVID-19) survival, *Clin. Infect. Dis.* 74 (2022) 1081–1084, <https://doi.org/10.1093/cid/ciab623>.
- [27] J.M. Audsley, N.E. Holmes, F.L. Mordant, C. Douros, S.E. Zufan, T.H.O. Nguyen, et al., Temporal differences in culturable severe acute respiratory coronavirus virus 2 (SARS-CoV-2) from the respiratory and gastrointestinal tracts in a patient with moderate coronavirus disease 2019 (COVID-19), *Infect. Control Hosp. Epidemiol.* 43 (2022) 1286–1288, <https://doi.org/10.1017/ice.2021.223>.
- [28] H.W. Jeong, S.-M. Kim, H.-S. Kim, Y.-I. Kim, J.H. Kim, J.Y. Cho, et al., Viable SARS-CoV-2 in various specimens from COVID-19 patients, *Clin. Microbiol. Infect.* 26 (2020) 1520–1524, <https://doi.org/10.1016/j.cmi.2020.07.020>.
- [29] L. Jiao, H. Li, J. Xu, M. Yang, C. Ma, J. Li, et al., The gastrointestinal tract is an alternative route for SARS-CoV-2 infection in a nonhuman primate model, *Gastroenterology* 160 (2021) 1647–1661, <https://doi.org/10.1053/j.gastro.2020.12.001>.
- [30] F. Xiao, J. Sun, Y. Xu, F. Li, X. Huang, H. Li, et al., Infectious SARS-CoV-2 in Feces of patient with severe COVID-19, *Emerg. Infect. Dis.* 26 (2020) 1920–1922, <https://doi.org/10.3201/eid2608.200681>.
- [31] S.L. Bartlett, D.G. Diel, L. Wang, S. Zec, M. Laverack, M. Martins, et al., SARS-CoV-2 infection and longitudinal fecal screening in Malayan tigers (*Panthera tigris jacksoni*), Amur Tigers (*Panthera tigris altaica*), and African Lions (*Panthera leo krugeri*) at the Bronx Zoo, New York, USA, *J. Zoo. Wildl. Med.* 51 (2021) 733–744, <https://doi.org/10.1638/2020-0171>.
- [32] W. Wang, Y. Xu, R. Gao, R. Lu, K. Han, G. Wu, et al., Detection of SARS-CoV-2 in different types of clinical specimens, *JAMA* 323 (2020) 1843, <https://doi.org/10.1001/jama.2020.3786>.
- [33] Y. Zhang, C. Chen, Y. Song, S. Zhu, D. Wang, H. Zhang, et al., Excretion of SARS-CoV-2 through faecal specimens, *Emerg. Microbes Infect.* 9 (2020) 2501–2508, <https://doi.org/10.1080/22221751.2020.1844551>.
- [34] J. Zhou, C. Li, X. Liu, M.C. Chiu, X. Zhao, D. Wang, et al., Infection of bat and human intestinal organoids by SARS-CoV-2, *Nat. Med.* 26 (2020) 1077–1083, <https://doi.org/10.1038/s41591-020-0912-6>.
- [35] H. Yao, X. Lu, Q. Chen, K. Xu, Y. Chen, L. Cheng, et al., Patient-derived mutations impact pathogenicity of, 04.14.20060160. SARS-CoV 2 (2020) 2020, <https://doi.org/10.1101/2020.04.14.20060160>.
- [36] J.P. Crimaldi, A.C. True, K.G. Linden, M.T. Hernandez, L.T. Larson, A.K. Pauls, Commercial toilets emit energetic and rapidly spreading aerosol plumes, *Sci. Rep.* 12 (2022) 20493, <https://doi.org/10.1038/s41598-022-24686-5>.
- [37] NHS England and NHS Improvement, Specialised ventilation for healthcare premises, 2021.
- [38] Noakes C.J., Fletcher L.A., Sleigh P.A., Booth W.B., Beato-Arribas B., Tomlinson N. Comparison of Tracer Techniques for Evaluating the Behaviour of Bioaerosols in Hospital Isolation Rooms. 9th International Conference and Exhibition on Healthy Buildings 2009 (HB09), Syracuse: International Society of Indoor Air Quality and Climate (ISIAQ); 2009.
- [39] M.-F. King, M. Camargo-Valero, A. Matamoros-Veloz, P. Sleigh, C.J. Noakes, An effective surrogate tracer technique for *S. aureus* bioaerosols in a mechanically ventilated hospital room replica using dilute aqueous lithium chloride, *Atmosphere* 8 (2017) 238, <https://doi.org/10.3390/atmos8120238>.
- [40] BS 6465-2:2017, Sanitary Installations: Space Recommendations. Code of Practice, British Standards Institution, 2017.
- [41] D.N. Henning, Use of public washrooms in an enclosed, suburban shopping plaza. National Research Council of Canada, Division of Building Research, 1977, <https://doi.org/10.4224/20359222>.
- [42] S.K. Rawls, Restroom usage in selected public buildings and facilities: a comparison of females and males. Virginia Polytechnic Institute and State University 1988.
- [43] S.M.V. Gwynne, A.L.E. Hunt, J.R. Thomas, A.J.L. Thompson, L. Séguin, The toilet paper: bathroom dwell time observations at an airport, *J. Build. Eng.* 24 (2019) 100751, <https://doi.org/10.1016/j.job.2019.100751>.
- [44] M.A. Baillie, S. Fraser, M.J. Brown, Do women spend more time in the restroom than men? *Psychol. Rep.* 105 (2009) 789–790, <https://doi.org/10.2466/PRO.105.3.789-790>.
- [45] H.D. Johnson, D. Sholcosky, K. Gabello, R. Ragni, N. Ogonosky, Sex differences in public restroom handwashing behavior associated with visual behavior prompts, *Percept. Mot. Skills* 97 (2003) 805–810, <https://doi.org/10.2466/pms.2003.97.3.805>.
- [46] P.J. Davidson, R.G. Courtney, Revised scales for sanitary accommodation in offices, *Build. Environ.* 11 (1976) 51–56, [https://doi.org/10.1016/0360-1323\(76\)90019-6](https://doi.org/10.1016/0360-1323(76)90019-6).
- [47] U.S. Environmental Protection Agency, Washington, DC. Exposure Factors Handbook 2011 Edition (Final Report). 2011.
- [48] A.M. Wilson, K. Canter, S.E. Abney, C.P. Gerba, E.R. Myers, J. Hanlin, et al., An application for relating Legionella shower water monitoring results to estimated health outcomes, *Water Res.* 221 (2022) 118812, <https://doi.org/10.1016/j.watres.2022.118812>.
- [49] B.S. Binkowitz, D. Wartenberg, Disparity in quantitative risk assessment: a review of input distributions, *Risk Anal.* 21 (2001) 75–90, <https://doi.org/10.1111/0272-4332.211091>.
- [50] P. Foladori, F. Cutrupi, N. Segata, S. Manara, F. Pinto, F. Malpei, et al., SARS-CoV-2 from faeces to wastewater treatment: what do we know? *A review*, *Sci. Total Environ.* 743 (2020) 140444, <https://doi.org/10.1016/j.scitotenv.2020.140444>.
- [51] G.B. McBride, *Using Statistical Methods for Water Quality Management: Issues, Problems and Solutions*, John Wiley & Sons, 2005.
- [52] G.B. McBride, R. Stott, W. Miller, D. Bambic, S. Wuertz, Discharge-based QMRA for estimation of public health risks from exposure to stormwater-borne pathogens in recreational waters in the United States, *Water Res* 47 (2013) 5282–5297, <https://doi.org/10.1016/j.watres.2013.06.001>.
- [53] A.C. Dada, P. Gyawali, Quantitative microbial risk assessment (QMRA) of occupational exposure to SARS-CoV-2 in wastewater treatment plants, *Sci. Total Environ.* 763 (2021) 142989, <https://doi.org/10.1016/j.scitotenv.2020.142989>.
- [54] N. Lee, M.C.W. Chan, B. Wong, K.W. Choi, W. Sin, G. Lui, et al., Fecal viral concentration and diarrhea in norovirus gastroenteritis, *Emerg. Infect. Dis.* 13 (2007) 1399–1401, <https://doi.org/10.3201/eid1309.061535>.
- [55] D.M. Brown, D. Butler, N.R. Orman, J.W. Davies, Gross solids transport in small diameter sewers, *Water Sci. Technol.* 33 (1996) 25–30, [https://doi.org/10.1016/0273-1223\(96\)00366-6](https://doi.org/10.1016/0273-1223(96)00366-6).
- [56] A.K. Pitot, T.R. Julian, Community transmission of SARS-CoV-2 by surfaces: risks and risk reduction strategies, *Environ. Sci. Technol. Lett.* 8 (2021) 263–269, <https://doi.org/10.1021/acs.estlett.0c00966>.
- [57] R.E. Black, M.M. Levine, M.L. Clements, L. Cisneros, V. Daya, Treatment of experimentally induced enterotoxigenic *Escherichia coli* Diarrhea with trimethoprim, trimethoprim-sulfamethoxazole, or placebo, *Rev. Infect. Dis.* 4 (1982) 540–545, <https://doi.org/10.1093/clinids/4.2.540>.
- [58] F. Miura, M. Kitajima, R. Omori, Duration of SARS-CoV-2 viral shedding in faeces as a parameter for wastewater-based epidemiology: re-analysis of patient data using a shedding dynamics model, *Sci. Total Environ.* 769 (2021) 144549, <https://doi.org/10.1016/j.scitotenv.2020.144549>.
- [59] P.F.M. Teunis, F.H.A. Sukhrrie, H. Vennema, J. Bogerman, M.F.C. Beersma, M.P. G. Koopmans, Shedding of norovirus in symptomatic and asymptomatic infections, *Epidemiol. Infect.* 143 (2015) 1710–1717, <https://doi.org/10.1017/S095026881400274X>.
- [60] A. Božić, M. Kanduč, Relative humidity in droplet and airborne transmission of disease, *J. Biol. Phys.* 47 (2021) 1–29, <https://doi.org/10.1007/s10867-020-09562-5>.

- [61] C.N. Haas, J.B. Rose, C.P. Gerba. *Quantitative Microbial Risk Assessment*, first ed. Wiley, 2014.
- [62] C.N. Haas, Action levels for SARS-CoV-2 in air: preliminary approach, *Risk Anal.* 41 (2021) 705–709, <https://doi.org/10.1111/risa.13728>.
- [63] A.M. Wilson, M.-F. King, M. López-García, I.J. Clifton, J. Proctor, K.A. Reynolds, et al., Effects of patient room layout on viral accrual on healthcare professionals' hands, *Indoor Air* 31 (2021) 1657–1672, <https://doi.org/10.1111/ina.12834>.
- [64] N. Van Abel, M.E. Schoen, J.C. Kissel, J.S. Meschke, Comparison of risk predicted by multiple norovirus dose–response models and implications for Quantitative Microbial Risk Assessment, *Risk Anal.* 37 (2017) 245–264, <https://doi.org/10.1111/risa.12616>.
- [65] E. Viau, K. Bibby, T. Paez-Rubio, J. Peccia, Toward a consensus view on the infectious risks associated with land application of sewage sludge, *Environ. Sci. Technol.* 45 (2011) 5459–5469, <https://doi.org/10.1021/es200566f>.
- [66] S.E. Abney, C.A. Higham, A.M. Wilson, M.K. Ijaz, J. McKinney, K.A. Reynolds, et al., Transmission of viruses from restroom use: a Quantitative Microbial Risk Assessment, *Food Environ. Virol.* 16 (2024) 65–78, <https://doi.org/10.1007/s12560-023-09580-1>.
- [67] J. Barker, S.F. Bloomfield, Survival of Salmonella in bathrooms and toilets in domestic homes following salmonellosis, *J. Appl. Microbiol.* 89 (2000) 137–144, <https://doi.org/10.1046/j.1365-2672.2000.01091.x>.
- [68] K. Pillay, L.C. Marr, A. Henriques, A.R. Martin, A.J. Prussin, L. Aleixo, et al., Can we use viral receptor mapping and particle deposition models to predict the clinical severity of novel airborne pathogens? *Clin. Microbiol. Infect.* 0 (2024) <https://doi.org/10.1016/j.cmi.2024.11.005>.
- [69] P. Azimi, Z. Keshavarz, J.G. Cedeno Laurent, B. Stephens, J.G. Allen, Mechanistic transmission modeling of COVID-19 on the diamond princess cruise ship demonstrates the importance of aerosol transmission, *Proc. Natl. Acad. Sci. USA* 118 (2021) e2015482118, <https://doi.org/10.1073/pnas.2015482118>.
- [70] H. Lei, Y. Li, S. Xiao, C.-H. Lin, S.L. Norris, D. Wei, et al., Routes of transmission of influenza A H1N1, SARS CoV, and norovirus in air cabin: comparative analyses, *Indoor Air* 28 (2018) 394–403, <https://doi.org/10.1111/ina.12445>.
- [71] A.R. Kolli, T.Z. Semren, D. Bovard, S. Majeed, M. van der Toorn, S. Scheuner, et al., Pulmonary delivery of aerosolized chloroquine and hydroxychloroquine to treat COVID-19: in vitro experimentation to human dosing predictions, *AAPS J.* 24 (2022) 33, <https://doi.org/10.1208/s12248-021-00666-x>.
- [72] M. Tan, Y. Tian, D. Zhang, Q. Wang, Z. Gao, Aerosol transmission of norovirus, *Viruses* 16 (2024) 151, <https://doi.org/10.3390/v16010151>.
- [73] M. Olsen, A. Lohning, M. Campos, P. Jones, S. McKirdy, R. Alghafri, et al., Mobile phones of paediatric hospital staff are never cleaned and commonly used in toilets with implications for healthcare nosocomial diseases, *Sci. Rep.* 11 (2021) 12999, <https://doi.org/10.1038/s41598-021-92360-3>.